

OAL: Enhancing OOD Detection Using Latent Diffusion

Heng Gao¹, Zhuolin He¹, Shoumeng Qiu¹, Jian Pu^{1*}

¹Fudan University

{hgao22, zlhe22}@m.fudan.edu.cn, skyshoumeng@163.com, jianpu@fudan.edu.cn

Abstract

Numerous Out-of-Distribution (OOD) detection algorithms have been developed to identify unknown samples or objects in real-world model deployments. Outlier Exposure (OE) algorithms, a subset of these methods, typically employ auxiliary datasets to train OOD detectors, enhancing the reliability of their predictions. While previous methods have leveraged Stable Diffusion (SD) to generate pixel-space outliers, these can complicate network optimization. We propose an Outlier Aware Learning (OAL) framework, which synthesizes OOD training data directly in the latent space. To regularize the model’s decision boundary, we introduce a mutual information-based contrastive learning approach that amplifies the distinction between In-Distribution (ID) and collected OOD features. The efficacy of this contrastive learning technique is supported by both theoretical analysis and empirical results. Furthermore, we integrate knowledge distillation into our framework to preserve in-distribution classification accuracy. The combined application of contrastive learning and knowledge distillation substantially improves OOD detection performance, enabling OAL to outperform other OE methods by a considerable margin. Source code is available at: <https://github.com/HengGao12/OAL>.

Introduction

Out-of-Distribution (OOD) detection is a crucial component for deploying models in the real world (Yang et al. 2024), and it has drawn increasing attention in the machine learning safety community. To prevent modern neural networks from being over-confident for OOD inputs and producing untrustworthy predictions (Nguyen, Yosinski, and Clune 2015), several studies proposed training the model with an auxiliary dataset (Hendrycks, Mazeika, and Dietterich 2019) and regularizing the model to learn a compact decision boundary between in-distribution and out-of-distribution data (Lee et al. 2018; Du et al. 2022c, 2023). These methods demonstrate superior OOD detection performance in comparison to those that do not utilize auxiliary datasets. While the main challenges for outlier exposure-based methods include: (i) collecting representative OOD samples for training, and (ii) effectively regularizing the model using the combination of ID and OOD data.

*Corresponding author.

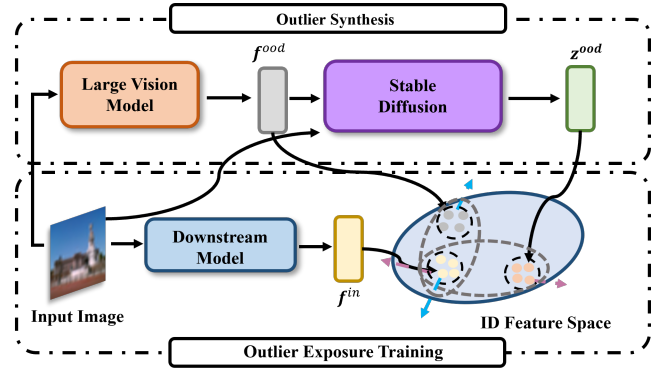


Figure 1: The illustration of the intuition behind the contrastive learning part in our OAL framework. Here, f^{ood} is the OOD embeddings sampled from a large model’s feature space by k-Nearest Neighbor (k-NN) (Kramer and Kramer 2013), z^{ood} is the latent representation generated by Diffusion conditioned by f^{ood} , f^{in} denotes the in-distribution feature of the downstream model. We enlarge the discrepancy between f^{in} and f^{ood} , z^{ood} using contrastive learning objective functions, thereby effectively regularizing the model’s decision boundary.

In recent work, VOS (Du et al. 2022c) synthesizes outliers in the feature space and directly uses these OOD data to regularize the model. Dream-OOD (Du et al. 2023) first proposed leveraging Stable Diffusion (Rombach et al. 2022) to generate photo-realistic OOD samples in the pixel space, marking a milestone in OOD detection. However, as empirically shown in VOS (Du et al. 2022c), synthesizing images in the high dimensional pixel space can be difficult to optimize (Yang et al. 2024). Therefore, it is natural to design a method that uses diffusion models to generate outliers in the latent space. Moreover, as demonstrated by our experiments in Figure 2, we find that the ID accuracy may decrease after introducing the collected OOD samples for training, even though the mean AUROC is improved. Nevertheless, the process of OOD detection must not compromise the in-distribution classification accuracy (Yang et al. 2024).

Motivated by these observations, we develop an Outlier

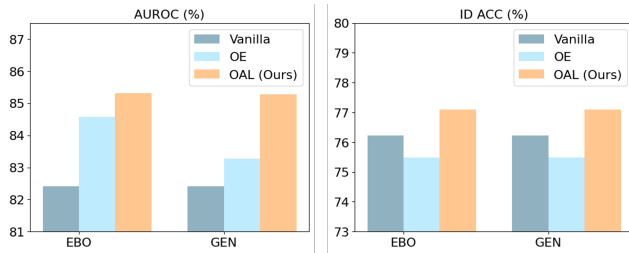


Figure 2: Performance comparisons. Here we compare the mean AUROC and ID accuracy of EBO (Liu et al. 2020) and GEN (Liu, Lochman, and Zach 2023) scores on CIFAR-100 benchmark using the vanilla training, the OE training and OAL training (Ours). The configuration of the OOD datasets is detailed in our experiments.

Aware Learning (OAL) framework that collects and learns with OOD data *in the latent space*. Specifically, we first use the k-NN (Kramer and Kramer 2013) to sample class-conditional outliers from the penultimate layer of Transformers (Dosovitskiy et al. 2020) encoders. Then, we take these outliers as token conditions for Stable Diffusion to generate OOD Latent embeddings for outlier exposure training. The main idea here is using the high-frequency and intricate details within the low-dimensional latent space of Stable Diffusion to benefit the feature-level training. To regularize the model’s decision boundary using these synthetic OOD data during training, we develop a mutual information-based feature contrastive learning approach that enlarges the discrepancy between the ID and OOD data. Both theoretical and experimental guarantees are provided for our contrastive learning method.

Besides, we introduce a simple yet effective knowledge distillation method into our learning framework to prevent the degradation of ID accuracy and increase supervision from ID data when performing outlier exposure training. Our experiments on CIFAR-10 and CIFAR-100 (Krizhevsky 2009) benchmarks achieve non-trivial improvement in OOD detection performance.

The main contributions of our paper can be summarized as follows:

- We propose the Outlier Aware Learning (OAL) framework, which generates OOD data from the latent space of Stable Diffusion, thereby facilitating network optimization during training using synthesized outliers.
- We develop a mutual information-based feature contrastive learning method to regularize the model’s decision boundary and propose a knowledge distillation approach to preserve ID classification performance.
- Our experiments demonstrate that the integration of contrastive learning and knowledge distillation achieves significant improvement in several metrics (FPR95, AUROC) using EBO score on CIFAR-10/100 benchmarks.

Related Work

Outlier exposure-based OOD detection. The key to outlier exposure-based approaches is to train the model by collecting Out-of-Distribution (OOD) samples, thereby improving the model’s ability to discern between In-Distribution (ID) and OOD data. In the basic OE algorithm (Hendrycks, Mazeika, and Dietterich 2019), they propose using an auxiliary dataset as the outlier data for training the OOD detector, which in turn improves its OOD detection performance. VOS (Du et al. 2022c) proposes to sample OOD data from a class-conditional distribution in the latent space to regularize the decision boundary between the ID data and the synthesized OOD data. Similarly, NPOS (Tao et al. 2023) also proposes to sample outliers in the latent space. Specifically, they do not make any distributional assumptions on the ID embeddings and generate synthetic outliers by adding Gaussian perturbations with rejection sampling in a CLIP-based embedding space. In Dream-OOD (Du et al. 2023), a method for outlier synthesis based on Stable Diffusion (Rombach et al. 2022) is proposed, which generates OOD samples in the pixel space. Different from Dream-OOD (Du et al. 2023), we synthesize outliers from the latent space of the Diffusion model, which facilitates the training of the model.

Representation learning-based OOD detection. The motivation for the representation learning-based method is to improve the representation ability of the model, thereby enhancing OOD detection performance. Sehwag et al. (Sehwag, Chiang, and Mittal 2021) and Winkens et al. (Winkens et al. 2020) empirically demonstrate the effectiveness of representation learning techniques in OOD detection through contrastive learning methods. CSI (Tack et al. 2020) contrasts samples with distributionally-shifted augmentations of themselves and introduce a new detection score adapted to this learning framework. SIREN (Du et al. 2022a) develop a trainable loss function to shape the representation into a mixture of vMF distribution (Mardia and Jupp 2009) on the unit hypersphere and propose a new OOD score based on the learned class-conditional vMF distributions. In our research, we explore the untapped potential of knowledge distillation in the context of OOD detection, verifying its effectiveness in both preventing ID accuracy degradation and enhancing OOD detection performance.

Diffusion models in OOD detection. Inspired by non-equilibrium thermodynamics, the Diffusion Probabilistic Model (DPM) was proposed to model the data distribution that enables precise sampling and evaluation of probabilities (Sohl-Dickstein et al. 2015). Afterwards, plenty of variants of the DPM have been proposed, such as DDPM (Ho, Jain, and Abbeel 2020), NCSNs (Song and Ermon 2019), DDPM++ (Song et al. 2021) and so forth. Nowadays, DPM has achieved great successes in many sorts of vision tasks, including image generation (Saharia et al. 2022; Dockhorn, Vahdat, and Kreis 2022), image inpainting (Cao, Dong, and Fu 2023; Lugmayr et al. 2022) and image segmentation (Wolleb et al. 2022; Chen et al. 2023), etc. In the respect of OOD detection, many researchers propose to use diffusion models to perform outlier detection. For instance, in (Graham et al. 2023), the authors apply DDPMs to perform unsupervised OOD detection, which leverages the reconstruction error metrics to

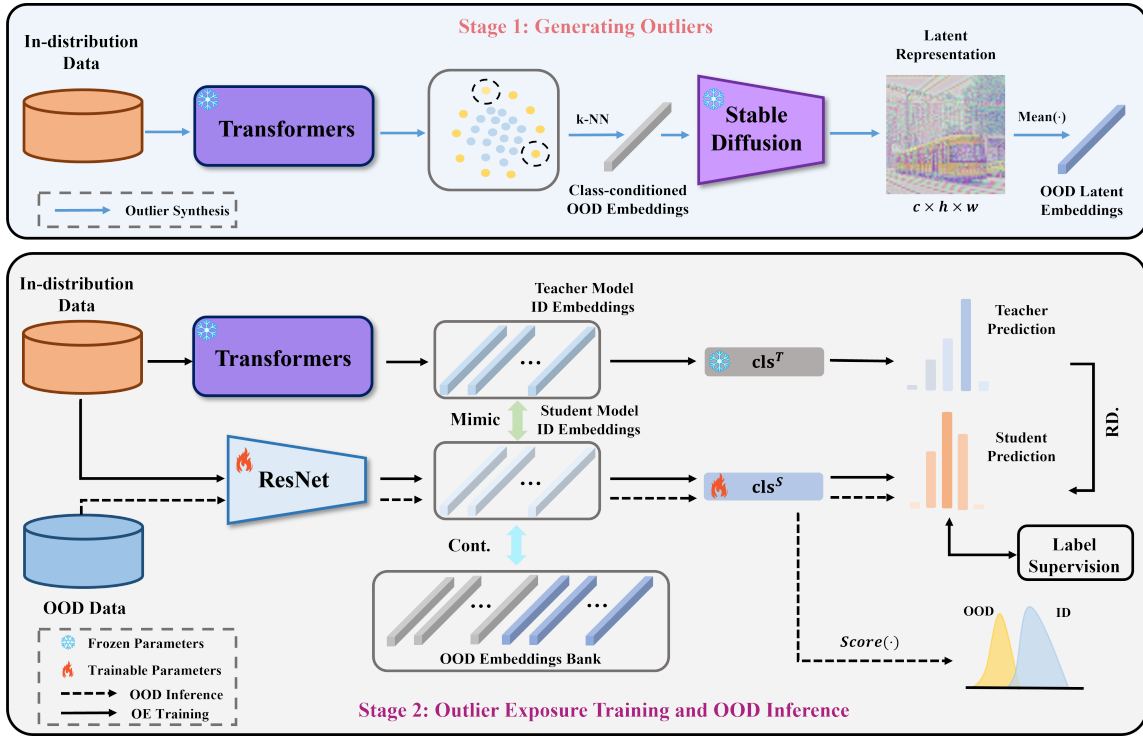


Figure 3: The overview of our OAL training pipeline for enhancing OOD detection. ‘Cont.’ represents the contrastive learning module in our framework. ‘RD.’ denotes response distillation. $Score(\cdot)$ denotes the score function used in the OOD inference phase.

confirm whether an image is OOD. DIFFGUARD (Graham et al. 2023) uses the guidance from semantic mismatch to better discern ID samples from the OOD ones. LMD (Liu et al. 2023) utilizes the diffusion model’s manifold mapping ability to conduct unsupervised OOD detection. In this study, we explore the application of Stable Diffusion (Rombach et al. 2022) in generating latent-based OOD data for outlier exposure training.

Methodology

Our OAL training framework is shown in Figure 3. In brief, it primarily addresses the following issues: (1) how to effectively collect and train with outliers by using Stable Diffusion; (2) how to mitigate the degradation of ID performance when training with the collected OOD data. The whole workflow of OAL consists of 2 stages. In Stage 1, we use the ID embeddings extracted from a pre-trained teacher model for k-NN to sample class-conditioned OOD embeddings. Then, we use Stable Diffusion (Rombach et al. 2022) to further generate OOD latent embeddings for OE training. In Stage 2, we develop a series of learning algorithms based on knowledge distillation and contrastive learning to effectively learn from these OOD data. Finally, we use the model trained by OAL to conduct OOD inference. In the following sections, we will introduce our framework with equations and reveal more details of our contributions.

Preliminaries

Let \mathcal{X} denote the in-distribution input image space, $\mathcal{Y} = \{1, 2, \dots, C\}$ denote the label space. We consider the multi-classification task using a standard dataset denoted by $\mathcal{D} = \{(\mathbf{x}_i, y_i)\}_{i=1}^N$, which is drawn *i.i.d.* from the joint data distribution $P_{\mathcal{X}\mathcal{Y}}^{in}$, where N is the number of samples, $\mathbf{x}_i \in \mathcal{X}$, $y_i \in \mathcal{Y}$, $i = 1, \dots, N$.

OOD detection. When deploying a machine learning model in the real world, a reliably classifier should not only classify ID samples, but also accurately identify OOD samples. Formally, given a test sample \mathbf{x} and a pre-trained classifier $f(\cdot)$, an OOD detection decision function can be written as

$$\mathcal{G}_\lambda(\mathbf{x}) = \begin{cases} \text{ID}, & S(\mathbf{x}) \geq \alpha, \\ \text{OOD}, & S(\mathbf{x}) < \alpha, \end{cases}$$

where α is the threshold, ID means that sample \mathbf{x} comes from the in-distribution dataset and OOD means that the sample \mathbf{x} comes from the out-of-distribution dataset.

Stable Diffusion model. To make the computation and training of diffusion models more efficient, in (Rombach et al. 2022), the authors proposed using an encoder $\mathcal{E}(\cdot)$ to compress the input images into a latent representation $\mathbf{z} = \mathcal{E}(\mathbf{x})$, $\mathbf{z} \in \mathbb{R}^{c \times h \times w}$. Then, they use a decoder $\mathcal{D}(\cdot)$ to decode the latent representation \mathbf{z} to the image space, which can be formally written as $\hat{\mathbf{x}} = \mathcal{D}(\mathbf{z})$. In our practical use, we synthesize OOD images by using the text prompts’

embeddings of label $y \in \mathcal{Y}$ for guidance.

Latent Space Outlier Synthesis

To synthesize OOD data in the latent space for training models without making any distributional assumptions, we develop a method that leverages k-NN and SD to generate various OOD embeddings. These embedding vectors serve as an auxiliary dataset for outlier exposure training, thereby improving the OOD detection performance.

Class-conditioned OOD features sampled by k-NN. We first use k-NN to sample outliers directly from the ID feature extracted by vision transformers’ (Dosovitskiy et al. 2020) encoders.

Denote $\mathbb{Z} = (z_1, z_2, \dots, z_n)$ as the set of the normalized training data feature vectors. Then, for any $z' \in \mathbb{Z}$, we calculate the k-NN distance, that is,

$$d_k(z', z_k) = \|z' - z_k\|_2,$$

where z_k is the k-th nearest embedding vectors in \mathbb{Z} , and z_k^* is the vector with max k-NN distance. We regard z_k^* as the boundary point of ID data. Then we use $\hat{z}_k^* := \|\mathcal{T}(c)\|_2 \cdot z_k^*$ as the center point of Gaussian kernels to sample class-conditioned OOD features, wherein $\mathcal{T}(c)$ is the text embedding of the name of class c in the classification task. In the end, we apply the k-NN distance again and select the k points that are farthest from the boundary points of \mathbb{Z} as the results of k-NN sampling.

OOD latent embeddings synthesis. To further enrich the diversity of OOD samples used in our training phase, we generate OOD Latent Embeddings from the latent space of Stable Diffusion.

Accordingly, we replace the token input of the Stable Diffusion’s text encoder with outlier embeddings \mathbf{v} obtained from the previous k-NN sampling. Then we leverage Stable Diffusion to generate OOD latent representations \mathbf{z}^{ood} conditioned on \mathbf{v} , which can be written as follows:

$$\mathbf{z}^{ood} \sim \tilde{P}(\mathbf{x}|\mathbf{v}),$$

where $\mathbf{z}^{ood} \in \mathbb{R}^{c \times h \times w}$, c is the number of channels, h is the height of the generated latent representations, w is the width of the generated representations, \mathbf{x} is the input image, $\tilde{P}(\mathbf{x}|\mathbf{v})$ is the \mathbf{v} conditioned latent space distribution. After the generation step, we average the first two dimensions of \mathbf{z}^{ood} and obtain the final OOD latent embedding

$$f^{ood} = \text{Mean}(\mathbf{z}^{ood}), \quad (1)$$

to train the model. In equation (1), $\text{Mean}(\cdot)$ denotes the operator that takes the average of the first two dimensions of \mathbf{z}^{ood} .

OOD Aware Model Regularization

To regularize the model’s decision boundary between ID and OOD features, we develop a contrastive learning and knowledge distillation-based approach to train the model using the synthesized OOD data.

Contrastive representation learning. After obtaining all these OOD features mentioned above, inspired by CLUB (Cheng et al. 2020), we develop a mutual information-based

outlier aware contrastive learning approach to enlarge the discrepancy between ID and OOD feature distribution in semantic space. To be specific, we propose a learning technique that minimizes the upper bound of mutual information between ID and OOD features. Different from (Cheng et al. 2020), our method is an extension of their theory from the logits case to the feature case. Furthermore, we verify the non-trivial benefits of the OOD detection performance of our method in the experiments.

We use mutual information to quantify the distance between the ID and OOD feature distribution, which takes the form as follows,

$$I(f_S^{in}, f_T^{ood}) = \mathbb{E}_{p(f_S^{in}, f_T^{ood})} \left[\log \frac{p(f_S^{in}, f_T^{ood})}{p(f_S^{in}) p(f_T^{ood})} \right],$$

where $f_S^{in} \in \mathbb{R}^m$ is the penultimate layer’s feature of the student network, $f_T^{ood} \in \mathbb{R}^n$ denotes the OOD embeddings synthesized by k-NN and Stable Diffusion. The mutual information loss function can be written as

$$\begin{aligned} \mathcal{L}_{MI}(f_S^{in}; f_T^{ood}) &:= \hat{I}(f_S^{in}, f_T^{ood}) \\ &= \mathbb{E}_{p(f_S^{in}, f_T^{ood})} [\log p(f_T^{ood} | f_S^{in})] - \\ &\quad \mathbb{E}_{p(f_S^{in})} \mathbb{E}_{p(f_T^{ood})} [\log p(f_T^{ood} | f_S^{in})]. \end{aligned} \quad (2)$$

Indeed, one can easily show that $\hat{I}(f_S^{in}, f_T^{ood})$ is an upper bound of $I(f_S^{in}, f_T^{ood})$.

Theorem 1. $\hat{I}(f_S^{in}, f_T^{ood})$ is an upper bound of $I(f_S^{in}, f_T^{ood})$.

In addition, we can show that the usage of the mutual information upper bound loss (2) for contrastive learning is not affected by the precision of upper bound estimates. This fact can be verified by **Theorem 2**.

Theorem 2. Denote $I_{sup}(f_S^{in}, f_T^{ood})$ as the supremum of $I(f_S^{in}, f_T^{ood})$. Then, there exists $M > 0$, s.t., for any sample size $m > M$, it is equivalent to using I_{sup} or \hat{I} as the loss function to regularize the student network.

Detailed proof of **Theorem 1** and **Theorem 2** are given in the supplementary materials. We also give the empirical validation for **Theorem 2**.

Knowledge distillation for ID performance boosting. Besides using mutual information-based loss function to enlarge feature discrepancies, we also develop simple yet effective knowledge distillation approaches to prevent in-distribution classification accuracy from degradation and further enhance OOD detection performance.

We directly apply KL divergence loss function to allow the student network to mimic the teacher network’s logits outputs, which can be formulated as follows:

$$\mathcal{L}_{KL}^1(y^S, y^T) = \int_{\mathbf{x} \in \mathcal{X}} \ln \left(\frac{y^S}{y^T} \right) y^S d\mathbf{x},$$

where y^S is the logits prediction of the student network, y^T is the prediction of the teacher model, y^{gt} is the ground truth, f_S^{in} is the in-distribution feature of student model, f_T^{in} is the ID feature extracted by teacher model.

Table 1: Evaluation using CIFAR-100 as the in-distribution dataset. We report standard deviations across 3 runs for the outlier synthesis-based methods. The bold numbers represent the best results.

Methods	Near-OOD CIFAR-10		MNIST		Far-OOD		SVHN		Average		ID ACC
	FPR@95 ↓	AUROC ↑	FPR@95 ↓	AUROC ↑	FPR@95 ↓	AUROC ↑	FPR@95 ↓	AUROC ↑			
Post hoc-based											
MSP (Hendrycks and Gimpel 2017)	58.66	78.88	48.37	80.25	46.91	84.38	51.31	81.17	76.22		
ODIN (Liang, Li, and Srikant 2018)	61.22	77.85	35.20	88.01	54.39	80.81	50.27	82.22	76.22		
Gram (Sastry and Oore 2020)	92.94	50.30	94.72	41.75	11.47	97.51	66.38	63.19	76.22		
EBO (Liu et al. 2020)	60.84	78.43	46.43	81.36	38.73	87.48	48.67	82.42	76.22		
ReAct (Sun, Guo, and Li 2021)	71.14	73.38	58.37	77.55	34.28	89.22	54.60	80.05	75.36		
ViM (Wang et al. 2022)	65.58	70.96	56.06	74.05	63.04	69.03	61.56	71.35	76.22		
KNN (Sun et al. 2022)	71.80	76.19	46.34	84.69	56.16	85.12	58.10	82.00	76.22		
GEN (Liu, Lochman, and Zach 2023)	60.82	78.44	46.44	81.36	38.76	87.47	48.67	82.42	76.22		
Outlier Exposure-based											
OE (Hendrycks, Mazeika, and Dietterich 2019)	65.78	77.14	37.13	87.96	37.82	88.63	46.91	84.57	75.49		
VOS (Du et al. 2022c)	63.42±1.21	77.97±1.00	43.55±10.50	84.57±4.15	52.43±8.01	82.45±3.77	53.14±3.73	81.66±1.57	75.50±1.49		
OAL (Ours)	61.50±1.34	79.25±0.30	35.73±3.27	90.25±0.72	43.41±4.11	86.45±2.07	46.88±1.06	85.32±0.53	77.09±0.43		

Table 2: Comparisons using CIFAR-10 as the in-distribution dataset. We report standard deviations across 3 runs for the outlier synthesis-based methods. The bold numbers represent the best results.

Methods	Near-OOD CIFAR-100		MNIST		Far-OOD SVHN		Average		ID ACC
	FPR@95 ↓	AUROC ↑	FPR@95 ↓	AUROC ↑	FPR@95 ↓	AUROC ↑	FPR@95 ↓	AUROC ↑	
Post hoc-based									
MSP (Hendrycks and Gimpel 2017)	34.81	89.52	22.74	92.94	16.81	94.48	24.79	92.31	94.66
ODIN (Liang, Li, and Srikant 2018)	47.94	87.87	10.77	97.52	24.26	94.38	27.66	93.26	94.66
Gram (Sastry and Oore 2020)	86.66	64.63	86.82	46.07	10.64	97.60	61.37	69.43	94.66
EBO (Liu et al. 2020)	34.40	90.65	19.68	94.74	12.27	96.59	22.12	93.99	94.66
ReAct (Sun, Guo, and Li 2021)	40.78	89.67	23.13	94.06	14.63	96.05	26.18	93.26	94.64
ViM (Wang et al. 2022)	37.39	88.74	17.06	95.84	21.52	91.19	25.32	91.92	94.66
KNN (Sun et al. 2022)	37.43	89.44	23.31	93.45	26.63	91.48	29.12	91.46	94.66
GEN (Liu, Lochman, and Zach 2023)	34.38	90.65	19.98	94.68	12.70	96.53	22.35	93.95	94.66
Outlier Exposure-based									
OE (Hendrycks, Mazeika, and Dietterich 2019)	32.56	91.19	12.76	97.24	9.03	98.04	18.12	95.49	94.36
VOS (Du et al. 2022c)	34.76±0.35	90.52±0.18	16.86±4.53	95.62±1.20	12.60±1.34	96.49±0.49	21.40±1.05	94.21±0.19	94.19±0.18
OAL (Ours)	31.20±0.68	91.63±0.10	5.64±0.71	98.50±0.18	9.03±0.93	97.56±0.39	15.29±0.63	95.89±0.21	95.01±0.14

Then, to transfer ID information at the feature level, we use a domain transfer network consisting of a stack of Multi-Layer Perceptron (MLP) layers to align the feature spaces of the teacher model’s and student model’s penultimate layers. Formally, we denote the domain transfer network as $\text{MLP}(\cdot)$. The learning objective function for minimizing the distribution discrepancy between the teacher model’s feature and the student model’s feature can be written as follows:

$$\mathcal{L}_{KL}^2(f_S^{in}, f_T^{in}) = \int_{\mathbf{x} \in \mathcal{X}} \ln \left(\frac{f_S^{in}}{\text{MLP}(f_T^{in})} \right) f_S^{in} d\mathbf{x}.$$

In summary, the total loss function takes the form as:

$$\begin{aligned} \mathcal{L}_{total} = & \mathcal{L}_{CE}(y^S, y^{gt}) + \alpha_1 \mathcal{L}_{KL}^1(y^S, y^T) \\ & + \alpha_2 \mathcal{L}_{KL}^2(f_S^{in}, f_T^{in}) + \beta \mathcal{L}_{MI}(f_S^{in}, f_T^{ood}) \\ & + \gamma \mathcal{L}_{MI}(f_S^{in}, f_G^{ood}), \end{aligned} \quad (3)$$

where f_G^{ood} is the generated out-of-distribution embeddings through Stable Diffusion, $\alpha_1, \alpha_2, \beta, \gamma$ are the weights of each component of \mathcal{L}_{total} , \mathcal{L}_{CE} is the cross-entropy loss, \mathcal{L}_{KL}^1 is the KL-divergence loss for the logits output of student and teacher network, \mathcal{L}_{KL}^2 is the KL-divergence loss for the feature output of student and teacher network.

Experiments

Experimental Setup

Datasets. We evaluate our methods on two commonly used benchmarks: CIFAR-10 and CIFAR-100 (Krizhevsky 2009). We use these 2 datasets as the ID data to train our models. When using CIFAR-10 (Krizhevsky 2009) as the ID data, we take CIFAR-100 (Krizhevsky 2009), MNIST (Deng 2012), SVHN (Netzer et al. 2011) as the OOD datasets. When using CIFAR-100 (Krizhevsky 2009) as the ID dataset, we use CIFAR-10 (Krizhevsky 2009), MNIST (Deng 2012), SVHN (Netzer et al. 2011) as the OOD datasets.

Evaluation metrics. To evaluate the performance of OOD detection, we use 3 commonly used metrics: (i) the False Positive Rate (FPR) at 95% True Positive Rate; (ii) the Area Under the Receiver Operating Characteristic curve (AUROC); (iii) the in-distribution classification accuracy (ID ACC) of the tested models.

Implementation details. We choose ResNet-18 (He et al. 2016) as the backbone of the student model, ViT-B/16 (Dosovitskiy et al. 2020) as the backbone of the teacher model. Our models are all trained and evaluated using one NVIDIA Tesla V100 SMX2 32GB GPU. Our code is developed mainly based on OpenOOD (Zhang et al. 2024). To facilitate the usage of our knowledge distillation approaches, we set both

Table 3: Comparisons with other outlier synthesis-based methods using CIFAR-100 as the ID data. † denotes that the method is reproduced by ourselves. The reproduction details are given in our supplementary materials.

Methods	OOD Dataset SVHN		ID ACC
	FPR@95 ↓	AUROC ↑	
GAN (Lee et al. 2018)	89.45	66.95	70.12
ATOL† (Zheng et al. 2023)	73.90	85.02	73.18
Dream-OOD (Du et al. 2023)	58.75±0.60	87.01±0.10	78.94
OAL (Ours)	43.41±4.11	86.45±2.07	77.09±0.43

the train and test image resolution to 224×224 for all methods on CIFAR-10/100 (Krizhevsky 2009) benchmarks. For fairness, the train batch size of all methods is set to 128 and the validation and test batch size are set to 200. The batch size of the outlier data used for training is set to 256 for all OE-based approaches. For both CIFAR-10 and CIFAR-100 datasets (Krizhevsky 2009), the training epoch of our method is set to 100 and the learning rate is 0.005. The weights in loss function (3) for both CIFAR-10 and CIFAR-100 are set to $\alpha_1 = 4.0$, $\alpha_2 = 8.0$, $\beta = 0.1$, $\gamma = 0.2$, respectively. We generate 300 OOD latent embeddings using Stable Diffusion v1.4 using CIFAR-10/100 as the ID data. In addition, we do not apply any test time augmentation or data augmentation techniques.

Main Results

To verify the effectiveness of our methods, we apply OAL to the EBO (Liu et al. 2020) score function and test the method on CIFAR-100 and CIFAR-10 (Krizhevsky 2009) benchmarks. The other outlier exposure-based methods, listed in Tables 1 and 2 for comparison, are all tested using ResNet-18 as the backbone and EBO as the score function.

Evaluation on CIFAR-100. From Table 1, we can see that OAL outperforms the other outlier exposure-based methods, such as OE (Hendrycks, Mazeika, and Dietterich 2019) and VOS (Du et al. 2022c), as well as post-hoc methods with a certain margin. Notably, the standard deviation of the FPR@95 and the AUROC of our method across 3 runs is far lower than that of VOS (Du et al. 2022c), indicating that OAL is robust to changes in the synthesized OOD features used for training.

Evaluation on CIFAR-10. As shown in Table 2, OAL also achieves the best performance among all post-hoc based and outlier exposure-based approaches. It is surprising that the mean FPR@95 of OAL on MNIST (Deng 2012) achieves only 5.64%. Moreover, the mean FPR@95 of our method gets 9.03% on SVHN (Netzer et al. 2011).

Comparisons with other outlier synthesis-based approaches. Furthermore, we conduct comparisons between OAL and the other outlier synthesis-based methods, such as GAN (Lee et al. 2018), Dream-OOD (Du et al. 2022b), and ATOL (Zheng et al. 2023), in Table 3. We only use SVHN (Netzer et al. 2011) as the OOD dataset for comparison due to our OOD dataset configuration setting. As shown in Table 3, OAL’s mean FPR@95 is 15.34% lower than that of Dream-OOD’s on SVHN, which indicates that the feature

Table 4: Ablation of loss functions in OAL on the CIFAR-100 benchmark using EBO score.

	Dist.	Cont. OE	Deep Cont. OE	FPR@95 ↓	AUROC ↑	ID ACC
(i)	✗	✗	✗	48.67	82.42	76.22
(ii)	✓	✗	✗	50.27	82.42	76.16
(iii)	✓	✓	✗	49.94	83.21	77.51
(iv)	✗	✓	✓	51.14	81.66	75.91
(v)	✓	✓	✓	46.88±1.06	85.32±0.53	77.09±0.43

Table 5: Ablation analysis on the backbone, taking CIFAR-100 as the in-distribution dataset.

Backbone	Methods	Average		ID ACC
		FPR@95 ↓	AUROC ↑	
ResNet-18	EBO (Liu et al. 2020)	48.67	82.42	76.22
	+ OAL	46.88±1.06	85.32±0.53	77.09±0.43
ResNet-50	EBO (Liu et al. 2020)	60.38	78.46	75.16
	+ OAL	50.02±1.58	85.71±0.20	86.49±0.28

level outlier synthesis using Stable Diffusion is better than synthesizing in the pixel-space. This result further confirms the statement that pixel-level OOD data is not easy to optimize when performing outlier exposure training.

Ablation Study

Ablation of the learning framework. Here we investigate the impact of each component of our learning framework on the CIFAR-100 (Krizhevsky 2009) benchmark. The results are shown in Table 4. In Table 4, ‘Dist.’ denotes using feature and logits distillation for training. ‘Cont. OE’ denotes training with outliers sampled by k-NN using mutual information contrastive loss. ‘Deep Cont. OE’ represents using outliers generated by Diffusion for contrastive learning. The comparison between setting (iii) and setting (v) in Table 4 shows the effectiveness of using OOD data synthesized by Diffusion for outlier exposure training. Then, comparing setting (iv) and setting (v) in Table 4 we can observe that our knowledge distillation methods enhance the ID classification accuracy of the original EBO (Liu et al. 2020) and even have a positive impact on FPR@95 and AUROC.

More importantly, by observing setting (i), (ii), (iv) and (v), we can find that using knowledge distillation only or using generated OOD data for outlier exposure training only will not make any improvements on the final OOD detection performance, which indicates that the combination of knowledge distillation and contrastive learning methods significantly improves the OOD detection results. Moreover, it demonstrates that using only ID or OOD features for supervision may lead to performance decreases.

Ablation on the backbone. In this section, we analyze the impact of changes to the backbone. The results are shown in Table 5. From Table 5 we can find that OAL is effective for both ResNet-18 and ResNet-50 using EBO score as the OOD detector, verifying that OAL is robust to backbone change.

Ablation of score functions. To verify the versatility of our methods, we further apply OAL to MSP (Hendrycks and Gimpel 2017) and GEN (Liu, Lochman, and Zach 2023) (the

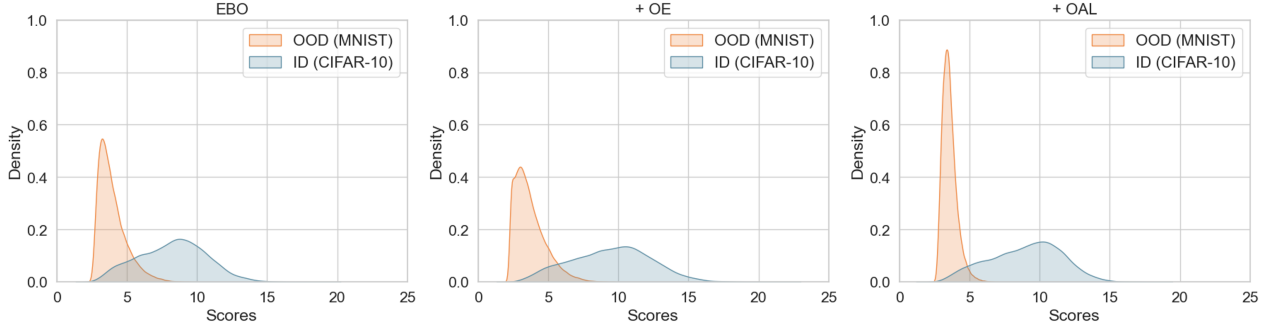


Figure 4: The score distribution visualization of EBO taking CIFAR-10 as the ID data, MNIST as the OOD data and ResNet-18 as the backbone.

Table 6: Ablation of the score function in our training framework on CIFAR-100 benchmark using ResNet-18 and EBO score.

Methods	Average		ID ACC
	FPR@95 ↓	AUROC ↑	
MSP (Hendrycks and Gimpel 2017)	51.31	81.17	76.22
+ OAL	54.87±0.96	81.92±0.31	77.09±0.43
EBO (Liu et al. 2020)	48.67	82.42	76.22
+ OAL	46.88±1.06	85.32±0.53	77.09±0.43
KNN (Sun et al. 2022)	58.10	82.00	76.22
+ OAL	59.68±1.72	80.91±1.16	77.09±0.43
GEN (Liu, Lochman, and Zach 2023)	48.67	82.42	76.22
+ OAL	46.98±1.17	85.28±0.51	77.09±0.43

softmax-based), KNN (Sun et al. 2022) (the distance-based) on the CIFAR-100 benchmark. As shown in Table 6, OAL works well for MSP (Hendrycks and Gimpel 2017), GEN (Liu, Lochman, and Zach 2023) scores and EBO (Liu et al. 2020) scores. But KNN’s (Sun et al. 2022) mean FPR@95 and AUROC decrease after using OAL for training the network. Therefore, our experiment results imply that OAL has a positive impact on the softmax-based, the energy-based methods and has negative impact on the distance-based scores.

Score Distribution Analysis

In this section, we aim to explore the effect of OAL training on the score distribution using EBO score. To this end, we visualize the score distribution of EBO using CIFAR-10 as the in-distribution data and MNIST as the OOD data under the vanilla training, the basic OE training, and our OAL training, respectively. As shown in Figure 4, we can find that OAL diminishes more overlap areas between the ID and OOD score distributions compared to OE on the MNIST dataset. This indicates that OAL has a stronger ability to enhance EBO’s OOD detection performance than OE. Besides, we can also find that the standard deviation of the estimated scores on both ID and OOD data is reduced considerably after applying OAL, highlighting another advantage of our method.

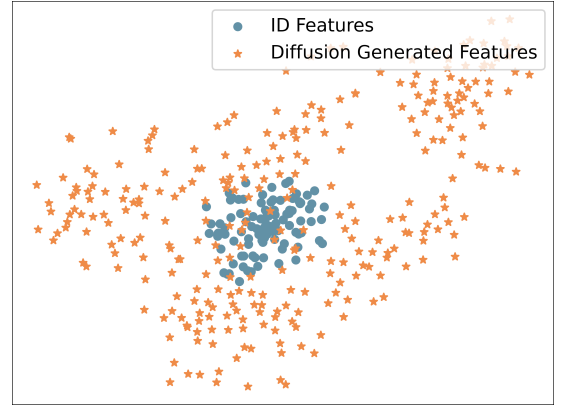


Figure 5: TSNE (Van der Maaten and Hinton 2008) visualization of the ID embeddings extracted by ViTs (the blue dots) and OOD latent representations synthesized by Stable Diffusion (the orange stars), for the class “lion” in CIFAR-100.

Visualization of the Synthesized Outliers

In this section, we visualize the synthesized OOD features using OAL in Figure 5. The ID features are extracted from the penultimate layer of a ViT-B/16 pre-trained on CIFAR-100. This fact demonstrates that, without making any distributional assumptions on either the ID or OOD feature space, OAL can generate outliers (the orange stars in Figure 5) in the low-likelihood region of the class “lion” (the blue dots in Figure 5). Therefore, OAL possesses a strong ability to enhance the model’s OOD detection performance.

Conclusion

In this work, we introduce OAL, a novel outlier exposure training framework designed to boost OOD detection performance. We facilitate model learning by synthesizing OOD features from the latent space of Stable Diffusion and employing a mutual information-based contrastive learning approach to effectively regularize the decision boundary between ID and OOD data. Moreover, we incorporate knowledge distil-

lation to prevent degradation in ID classification accuracy while simultaneously enhancing OOD detection. Our experiments demonstrate that the integration of these learning algorithms leads to significant improvements on the CIFAR-10/100 benchmarks.

References

- Cao, C.; Dong, Q.; and Fu, Y. 2023. Zits++: Image inpainting by improving the incremental transformer on structural priors. *IEEE Transactions on Pattern Analysis and Machine Intelligence*, 45(10): 12667–12684.
- Chen, J.; Lu, J.; Zhu, X.; and Zhang, L. 2023. Generative semantic segmentation. In *Proceedings of the IEEE/CVF Conference on Computer Vision and Pattern Recognition*, 7111–7120.
- Cheng, P.; Hao, W.; Dai, S.; Liu, J.; Gan, Z.; and Carin, L. 2020. Club: A contrastive log-ratio upper bound of mutual information. In *International conference on machine learning*, 1779–1788. PMLR.
- Deng, L. 2012. The mnist database of handwritten digit images for machine learning research [best of the web]. *IEEE signal processing magazine*, 29(6): 141–142.
- Dockhorn, T.; Vahdat, A.; and Kreis, K. 2022. Score-Based Generative Modeling with Critically-Damped Langevin Diffusion. In *International Conference on Learning Representations*.
- Dosovitskiy, A.; Beyer, L.; Kolesnikov, A.; Weissenborn, D.; Zhai, X.; Unterthiner, T.; Dehghani, M.; Minderer, M.; Heigold, G.; Gelly, S.; et al. 2020. An Image is Worth 16x16 Words: Transformers for Image Recognition at Scale. In *International Conference on Learning Representations*.
- Du, X.; Gozum, G.; Ming, Y.; and Li, Y. 2022a. Siren: Shaping representations for detecting out-of-distribution objects. *Advances in Neural Information Processing Systems*, 35: 20434–20449.
- Du, X.; Sun, Y.; Zhu, J.; and Li, Y. 2023. Dream the Impossible: Outlier Imagination with Diffusion Models. In Oh, A.; Naumann, T.; Globerson, A.; Saenko, K.; Hardt, M.; and Levine, S., eds., *Advances in Neural Information Processing Systems*, volume 36, 60878–60901. Curran Associates, Inc.
- Du, X.; Wang, X.; Gozum, G.; and Li, Y. 2022b. Unknown-Aware Object Detection: Learning What You Don’t Know from Videos in the Wild. In *Proceedings of the IEEE/CVF Conference on Computer Vision and Pattern Recognition*, 13678–13688.
- Du, X.; Wang, Z.; Cai, M.; and Li, S. 2022c. Towards Unknown-aware Learning with Virtual Outlier Synthesis. In *International Conference on Learning Representations*.
- Graham, M. S.; Pinaya, W. H.; Tudosi, P.-D.; Nachev, P.; Ourselin, S.; and Cardoso, J. 2023. Denoising diffusion models for out-of-distribution detection. In *Proceedings of the IEEE/CVF Conference on Computer Vision and Pattern Recognition*, 2948–2957.
- He, K.; Zhang, X.; Ren, S.; and Sun, J. 2016. Deep residual learning for image recognition. In *Proceedings of the IEEE conference on computer vision and pattern recognition*, 770–778.
- Hendrycks, D.; and Gimpel, K. 2017. A Baseline for Detecting Misclassified and Out-of-Distribution Examples in Neural Networks. In *International Conference on Learning Representations*.
- Hendrycks, D.; Mazeika, M.; and Dietterich, T. 2019. Deep Anomaly Detection with Outlier Exposure. In *International Conference on Learning Representations*.
- Ho, J.; Jain, A.; and Abbeel, P. 2020. Denoising diffusion probabilistic models. *Advances in neural information processing systems*, 33: 6840–6851.
- Kramer, O.; and Kramer, O. 2013. K-nearest neighbors. *Dimensionality reduction with unsupervised nearest neighbors*, 13–23.
- Krizhevsky, A. 2009. Learning Multiple Layers of Features from Tiny Images. *Citeseer*.
- Lee, K.; Lee, H.; Lee, K.; and Shin, J. 2018. Training Confidence-calibrated Classifiers for Detecting Out-of-Distribution Samples. In *International Conference on Learning Representations*.
- Liang, S.; Li, Y.; and Srikant, R. 2018. Enhancing The Reliability of Out-of-distribution Image Detection in Neural Networks. In *International Conference on Learning Representations*.
- Liu, W.; Wang, X.; Owens, J.; and Li, Y. 2020. Energy-based out-of-distribution detection. *Advances in neural information processing systems*, 33: 21464–21475.
- Liu, X.; Lochman, Y.; and Zach, C. 2023. GEN: Pushing the Limits of Softmax-Based Out-of-Distribution Detection. In *Proceedings of the IEEE/CVF Conference on Computer Vision and Pattern Recognition*, 23946–23955.
- Liu, Z.; Zhou, J. P.; Wang, Y.; and Weinberger, K. Q. 2023. Unsupervised out-of-distribution detection with diffusion inpainting. In *International Conference on Machine Learning*, 22528–22538. PMLR.
- Lugmayr, A.; Danelljan, M.; Romero, A.; Yu, F.; Timofte, R.; and Van Gool, L. 2022. Repaint: Inpainting using denoising diffusion probabilistic models. In *Proceedings of the IEEE/CVF conference on computer vision and pattern recognition*, 11461–11471.
- Mardia, K. V.; and Jupp, P. E. 2009. *Directional statistics*. John Wiley & Sons.
- Mohri, M.; Rostamizadeh, A.; and Talwalkar, A. 2018. *Foundations of machine learning*. MIT press.
- Morteza, P.; and Li, Y. 2022. Provable guarantees for understanding out-of-distribution detection. In *Proceedings of the AAAI Conference on Artificial Intelligence*, volume 36, 7831–7840.
- Netzer, Y.; Wang, T.; Coates, A.; Bissacco, A.; Wu, B.; Ng, A. Y.; et al. 2011. Reading digits in natural images with unsupervised feature learning. In *NIPS workshop on deep learning and unsupervised feature learning*, volume 2011, 4. Granada.
- Nguyen, A.; Yosinski, J.; and Clune, J. 2015. Deep neural networks are easily fooled: High confidence predictions for unrecognizable images. In *Proceedings of the IEEE conference on computer vision and pattern recognition*, 427–436.

Rombach, R.; Blattmann, A.; Lorenz, D.; Esser, P.; and Ommer, B. 2022. High-resolution image synthesis with latent diffusion models. In *Proceedings of the IEEE/CVF conference on computer vision and pattern recognition*, 10684–10695.

Saharia, C.; Chan, W.; Saxena, S.; Li, L.; Whang, J.; Denton, E. L.; Ghasemipour, K.; Gontijo Lopes, R.; Karagol Ayan, B.; Salimans, T.; et al. 2022. Photorealistic text-to-image diffusion models with deep language understanding. *Advances in neural information processing systems*, 35: 36479–36494.

Sastry, C. S.; and Oore, S. 2020. Detecting out-of-distribution examples with gram matrices. In *International Conference on Machine Learning*, 8491–8501. PMLR.

Sehwag, V.; Chiang, M.; and Mittal, P. 2021. {SSD}: A Unified Framework for Self-Supervised Outlier Detection. In *International Conference on Learning Representations*.

Sohl-Dickstein, J.; Weiss, E.; Maheswaranathan, N.; and Ganguli, S. 2015. Deep unsupervised learning using nonequilibrium thermodynamics. In *International conference on machine learning*, 2256–2265. PMLR.

Song, Y.; and Ermon, S. 2019. Generative Modeling by Estimating Gradients of the Data Distribution. In Wallach, H.; Larochelle, H.; Beygelzimer, A.; d'Alché-Buc, F.; Fox, E.; and Garnett, R., eds., *Advances in Neural Information Processing Systems*, volume 32. Curran Associates, Inc.

Song, Y.; Sohl-Dickstein, J.; Kingma, D. P.; Kumar, A.; Ermon, S.; and Poole, B. 2021. Score-Based Generative Modeling through Stochastic Differential Equations. In *International Conference on Learning Representations*.

Sun, Y.; Guo, C.; and Li, Y. 2021. React: Out-of-distribution detection with rectified activations. *Advances in Neural Information Processing Systems*, 34: 144–157.

Sun, Y.; Ming, Y.; Zhu, X.; and Li, Y. 2022. Out-of-distribution detection with deep nearest neighbors. In *International Conference on Machine Learning*, 20827–20840. PMLR.

Tack, J.; Mo, S.; Jeong, J.; and Shin, J. 2020. Csi: Novelty detection via contrastive learning on distributionally shifted instances. *Advances in neural information processing systems*, 33: 11839–11852.

Tao, L.; Du, X.; Zhu, J.; and Li, Y. 2023. Non-parametric Outlier Synthesis. In *The Eleventh International Conference on Learning Representations*.

Van der Maaten, L.; and Hinton, G. 2008. Visualizing data using t-SNE. *Journal of machine learning research*, 9(11).

Wang, H.; Li, Z.; Feng, L.; and Zhang, W. 2022. Vim: Out-of-distribution with virtual-logit matching. In *Proceedings of the IEEE/CVF conference on computer vision and pattern recognition*, 4921–4930.

Wei, H.; Xie, R.; Cheng, H.; Feng, L.; An, B.; and Li, Y. 2022. Mitigating neural network overconfidence with logit normalization. In *International Conference on Machine Learning*, 23631–23644. PMLR.

Winkens, J.; Bunel, R.; Roy, A. G.; Stanforth, R.; Natarajan, V.; Ledsam, J. R.; MacWilliams, P.; Kohli, P.; Karthikesalingam, A.; Kohl, S.; et al. 2020. Contrastive training for improved out-of-distribution detection. *arXiv preprint arXiv:2007.05566*.

Wolleb, J.; Sandkühler, R.; Bieder, F.; Valmaggia, P.; and Cattin, P. C. 2022. Diffusion models for implicit image segmentation ensembles. In *International Conference on Medical Imaging with Deep Learning*, 1336–1348. PMLR.

Yang, J.; Wang, H.; Feng, L.; Yan, X.; Zheng, H.; Zhang, W.; and Liu, Z. 2021. Semantically coherent out-of-distribution detection. In *Proceedings of the IEEE/CVF International Conference on Computer Vision*, 8301–8309.

Yang, J.; Zhou, K.; Li, Y.; and Liu, Z. 2024. Generalized out-of-distribution detection: A survey. *International Journal of Computer Vision*, 1–28.

Yu, Q.; and Aizawa, K. 2019. Unsupervised out-of-distribution detection by maximum classifier discrepancy. In *Proceedings of the IEEE/CVF international conference on computer vision*, 9518–9526.

Zhang, J.; Yang, J.; Wang, P.; Wang, H.; Lin, Y.; Zhang, H.; Sun, Y.; Du, X.; Zhou, K.; Zhang, W.; Li, Y.; Liu, Z.; Chen, Y.; and Li, H. 2024. OpenOOD v1.5: Enhanced Benchmark for Out-of-Distribution Detection. In *NeurIPS 2023 Workshop on Distribution Shifts: New Frontiers with Foundation Models*.

Zheng, H.; Wang, Q.; Fang, Z.; Xia, X.; Liu, F.; Liu, T.; and Han, B. 2023. Out-of-distribution Detection Learning with Unreliable Out-of-distribution Sources. In Oh, A.; Naumann, T.; Globerson, A.; Saenko, K.; Hardt, M.; and Levine, S., eds., *Advances in Neural Information Processing Systems*, volume 36, 72110–72123. Curran Associates, Inc.

Reproducibility Checklist

Unless specified otherwise, please answer “yes” to each question if the relevant information is described either in the paper itself or in a technical appendix with an explicit reference from the main paper. If you wish to explain an answer further, please do so in a section titled “Reproducibility Checklist” at the end of the technical appendix.

This paper:

- Includes a conceptual outline and/or pseudocode description of AI methods introduced [Yes]
- Clearly delineates statements that are opinions, hypothesis, and speculation from objective facts and results [Yes]
- Provides well marked pedagogical references for less-familiale readers to gain background necessary to replicate the paper [Yes]

Does this paper make theoretical contributions? [Yes]

If yes, please complete the list below.

- All assumptions and restrictions are stated clearly and formally. [Yes]
- All novel claims are stated formally (e.g., in theorem statements). [Yes]
- Proofs of all novel claims are included. [Yes]
- Proof sketches or intuitions are given for complex and/or novel results. [NA]
- Appropriate citations to theoretical tools used are given. [Yes]
- All theoretical claims are demonstrated empirically to hold. [Yes]

- All experimental code used to eliminate or disprove claims is included. [NA]

Does this paper rely on one or more datasets? [Yes]

If yes, please complete the list below.

- A motivation is given for why the experiments are conducted on the selected datasets [Yes] See the supplementary materials.
- All novel datasets introduced in this paper are included in a data appendix. [NA]
- All novel datasets introduced in this paper will be made publicly available upon publication of the paper with a license that allows free usage for research purposes. [NA]
- All datasets drawn from the existing literature (potentially including authors' own previously published work) are accompanied by appropriate citations. [Yes]
- All datasets drawn from the existing literature (potentially including authors' own previously published work) are publicly available. [Yes]
- All datasets that are not publicly available are described in detail, with explanation why publicly available alternatives are not scientifically satisfying. [NA]

Does this paper include computational experiments? [Yes]

If yes, please complete the list below.

- Any code required for pre-processing data is included in the appendix. [NA]
- All source code required for conducting and analyzing the experiments is included in a code appendix. [Yes]
- All source code required for conducting and analyzing the experiments will be made publicly available upon publication of the paper with a license that allows free usage for research purposes. [Yes]
- All source code implementing new methods have comments detailing the implementation, with references to the paper where each step comes from [Yes]
- If an algorithm depends on randomness, then the method used for setting seeds is described in a way sufficient to allow replication of results. [Yes]
- This paper specifies the computing infrastructure used for running experiments (hardware and software), including GPU/CPU models; amount of memory; operating system; names and versions of relevant software libraries and frameworks. [Yes]
- This paper formally describes evaluation metrics used and explains the motivation for choosing these metrics. [Yes]
- This paper states the number of algorithm runs used to compute each reported result. [Yes]
- Analysis of experiments goes beyond single-dimensional summaries of performance (e.g., average; median) to include measures of variation, confidence, or other distributional information. [Yes]
- The significance of any improvement or decrease in performance is judged using appropriate statistical tests (e.g., Wilcoxon signed-rank). [Yes]
- This paper lists all final (hyper-)parameters used for each model/algorithm in the paper's experiments. [Yes]

- This paper states the number and range of values tried per (hyper-) parameter during development of the paper, along with the criterion used for selecting the final parameter setting. [NA]

Appendix

Proof for Theorem 1

In this section, we give the detail calculation of our **Theorem 1** in the main paper.

Proof. Indeed, I and \hat{I} can be written as the following form,

$$\begin{aligned} I(f_S^{in}, f_T^{ood}) &= \mathbb{E}_{p(f_S^{in}, f_T^{ood})} \left[\log \frac{p(f_T^{ood} | f_S^{in})}{p(f_T^{ood})} \right], \\ \hat{I}(f_S^{in}, f_T^{ood}) &= \mathbb{E}_{p(f_S^{in}, f_T^{ood})} [\log p(f_T^{ood} | f_S^{in})] - \\ &\quad \mathbb{E}_{p(f_S^{in})} \mathbb{E}_{p(f_T^{ood})} [\log p(f_T^{ood} | f_S^{in})]. \end{aligned}$$

Denote

$$\Delta := \hat{I}(f_S^{in}, f_T^{ood}) - I(f_S^{in}, f_T^{ood}).$$

Then, we have

$$\begin{aligned} \Delta &= \mathbb{E}_{p(f_S^{in}, f_T^{ood})} [\log p(f_T^{ood} | f_S^{in})] \\ &\quad - \mathbb{E}_{p(f_S^{in})} \mathbb{E}_{p(f_T^{ood})} [\log p(f_T^{ood} | f_S^{in})] \\ &\quad - \mathbb{E}_{p(f_S^{in}, f_T^{ood})} \left[\log \frac{p(f_T^{ood} | f_S^{in})}{p(f_T^{ood})} \right] \\ &= \mathbb{E}_{p(f_S^{in}, f_T^{ood})} [\log p(f_T^{ood} | f_S^{in})] \\ &\quad - \mathbb{E}_{p(f_S^{in})} \mathbb{E}_{p(f_T^{ood})} [\log p(f_T^{ood} | f_S^{in})] \\ &\quad - \mathbb{E}_{p(f_S^{in}, f_T^{ood})} [\log p(f_T^{ood} | f_S^{in})] \\ &\quad + \mathbb{E}_{p(f_S^{in}, f_T^{ood})} [\log p(f_T^{ood})] \\ &= \mathbb{E}_{p(f_S^{in}, f_T^{ood})} [\log p(f_T^{ood})] \\ &\quad - \mathbb{E}_{p(f_S^{in})} \mathbb{E}_{p(f_T^{ood})} [\log p(f_T^{ood} | f_S^{in})] \\ &= \int_{\mathbb{R}^d} df_S^{in} \int_{\mathbb{R}^d} \log p(f_T^{ood}) p(f_S^{in}, f_T^{ood}) df_T^{ood} \\ &\quad - \mathbb{E}_{p(f_S^{in})} \mathbb{E}_{p(f_T^{ood})} [\log p(f_T^{ood} | f_S^{in})] \\ &= \int_{\mathbb{R}^d} \log p(f_T^{ood}) \left(\int_{\mathbb{R}^d} p(f_S^{in}, f_T^{ood}) df_S^{in} \right) df_T^{ood} - \\ &\quad \mathbb{E}_{p(f_S^{in})} \mathbb{E}_{p(f_T^{ood})} [\log p(f_T^{ood} | f_S^{in})] \end{aligned}$$

The above equations can be further written as

$$\begin{aligned} &\int_{\mathbb{R}^d} \log [p(f_T^{ood})] p(f_T^{ood}) df_T^{ood} - \\ &\int_{\mathbb{R}^d} p(f_S^{in}) df_S^{in} \int_{\mathbb{R}^d} \log [p(f_T^{ood} | f_S^{in})] p(f_T^{ood}) df_T^{ood} \\ &= \int_{\mathbb{R}^d} \log [p(f_T^{ood})] p(f_T^{ood}) df_T^{ood} - \\ &\int_{\mathbb{R}^d} p(f_T^{ood}) df_T^{ood} \int_{\mathbb{R}^d} \log [p(f_T^{ood} | f_S^{in})] p(f_S^{in}) df_S^{in} \\ &= \mathbb{E}_{p(f_T^{ood})} [\log p(f_T^{ood})] \\ &\quad - \mathbb{E}_{p(f_T^{ood})} [\mathbb{E}_{p(f_S^{in})} [\log p(f_T^{ood} | f_S^{in})]] \\ &= \mathbb{E}_{p(f_T^{ood})} [\log p(f_T^{ood}) - \mathbb{E}_{p(f_S^{in})} [\log p(f_T^{ood} | f_S^{in})]]. \end{aligned}$$

Then, according to the definition of the marginal distribution, we have,

$$\begin{aligned} p(f_T^{ood}) &= \int_{\mathbb{R}^d} p(f_T^{ood} | f_S^{in}) p(f_S^{in}) df_S^{in} \\ &= \mathbb{E}_{p(f_S^{in})} [p(f_T^{ood} | f_S^{in})]. \end{aligned}$$

Since $\forall x > 0, x > \log x$, therefore, we have

$$\begin{aligned} \Delta &= \mathbb{E}_{p(f_T^{ood})} [\log p(f_T^{ood}) - \mathbb{E}_{p(f_S^{in})} [\log p(f_T^{ood} | f_S^{in})]] \\ &= \mathbb{E}_{p(f_T^{ood})} [\log (\mathbb{E}_{p(f_S^{in})} [p(f_T^{ood} | f_S^{in})])] \\ &\quad - \mathbb{E}_{p(f_S^{in})} [\log p(f_T^{ood} | f_S^{in})]. \end{aligned}$$

Since $\log(\cdot)$ is a concave function and according to Jensen's inequality, we have

$$\begin{aligned} &\log (\mathbb{E}_{p(f_S^{in})} [p(f_T^{ood} | f_S^{in})]) \\ &\quad - \mathbb{E}_{p(f_S^{in})} [\log p(f_T^{ood} | f_S^{in})] \\ &= \log \int_{\mathbb{R}^d} p(f_T^{ood} | f_S^{in}) p(f_S^{in}) df_S^{in} \\ &\quad - \int_{\mathbb{R}^d} \log [p(f_T^{ood} | f_S^{in})] p(f_S^{in}) df_S^{in} \geq 0. \end{aligned}$$

Therefore, $\hat{I}(f_S^{in}, f_T^{ood})$ is an upper bound of $I(f_S^{in}, f_T^{ood})$.

Proof for Theorem 2

In this part, we give the detail proof of the **Theorem 2** in our main paper.

Proof. For simplicity, we first give the following assumptions (Mohri, Rostamizadeh, and Talwalkar 2018) to prove the theorem.

Assumption 1. Assume that the samples $S = (x_1, \dots, x_m)$ and the labels $(c(x_1), \dots, c(x_m))$ are identically distributed according to the ID data distribution \mathcal{D}^m , which follows Gaussian mixture distribution.

Now we assume that we only use the contrastive learning loss part in \mathcal{L}_{total} to train our model. In fact, the proof is similar to use all terms in \mathcal{L}_{total} .

Our task is to use the labeled sample S to learn a hypothesis $h_S \in \mathcal{H}$ that has a small generalization error with respect to concept c .

Define concept $c : \mathcal{X} \rightarrow \mathcal{Y}$ is a mapping from \mathcal{X} to \mathcal{Y} . A concept class \mathcal{C} is a set of concepts that we wish to learn.

The generalization error between the hypothesis h and the target concept $c \in \mathcal{C}$ underlying distribution \mathcal{D}^m can be written as

$$R(h) = \mathbb{P}_{x \sim \mathcal{D}^m} [h(x) \neq c(x)].$$

In the stochastic scenario case, the output label is a probabilistic function of the input. Thus, we use the following extension framework of PAC-learning to prove our theorem.

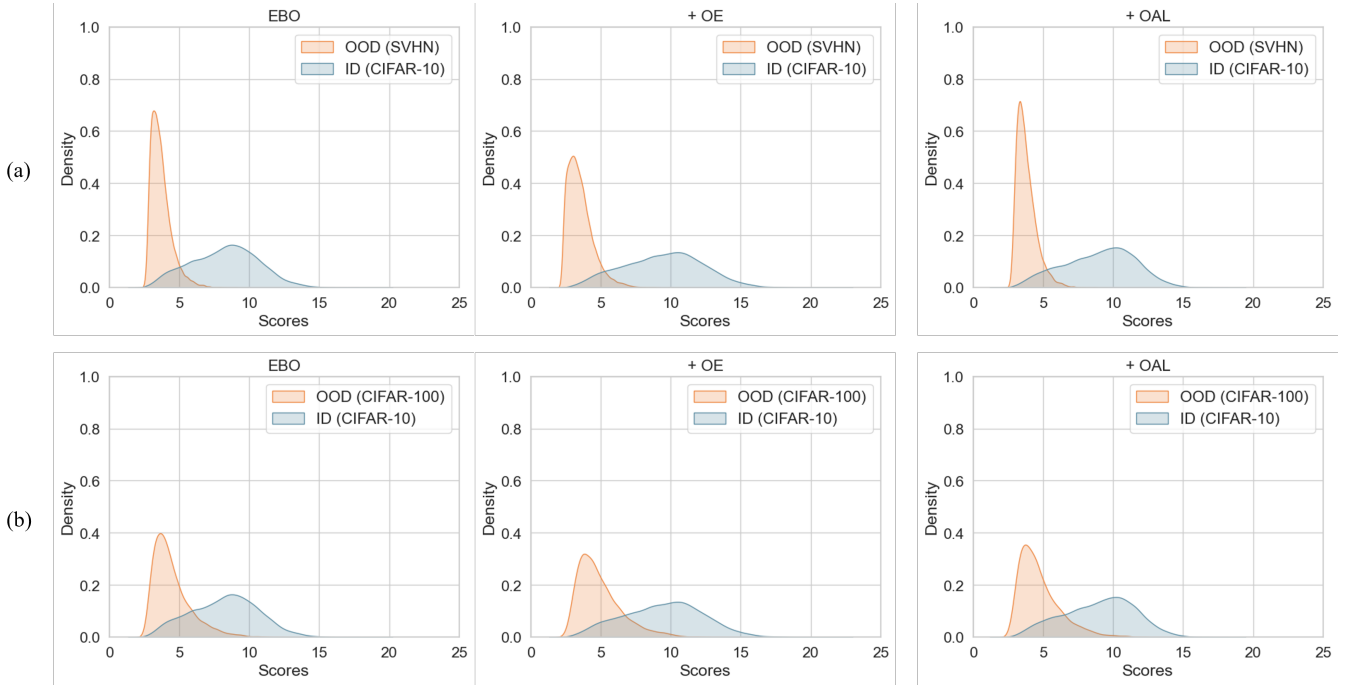


Figure A: The score distribution visualization of EBO (Liu et al. 2020) taking CIFAR-10 (Krizhevsky 2009) as the ID data, CIFAR-100 (Krizhevsky 2009) and SVHN (Netzer et al. 2011) as the OOD data and ResNet-18 (He et al. 2016) as the backbone.

Definition 1 (Agnostic PAC-learning). Let \mathcal{H} be a hypothesis set. \mathcal{A} is an agnostic PAC-learning algorithm if there exists a polynomial function $\text{poly}(\cdot, \cdot, \cdot, \cdot)$ such that for any $\varepsilon > 0, \delta > 0$, for all distributions \mathcal{D} over $\mathcal{X} \times \mathcal{Y}$, the following holds for any sample size $m > \text{poly}(1/\varepsilon, 1/\delta, n, \text{size}(c))$:

$$\mathbb{P}_{S \sim \mathcal{D}^m} [R(h_S) - \min_{h \in \mathcal{H}} R(h) \leq \varepsilon] \geq 1 - \delta.$$

If \mathcal{A} further runs in $\text{poly}(1/\varepsilon, 1/\delta, n, \text{size}(c))$, then it is said to be an efficient agnostic PAC-learning algorithm.

The advantage of using this definition is that the distribution \mathcal{D} can be arbitrary, which makes it well applied to any scenario.

Therefore, we denote $R(h_S)$ as the generalization error for using $\hat{I}(f_S^{\text{in}}, f_T^{\text{ood}})$, $R_{\text{sup}}(h_S)$ as the generalization error for using $I_{\text{sup}}(f_S^{\text{in}}, f_T^{\text{ood}})$. Furthermore, the algorithm is agnostic PAC-learnable when using \hat{I} and I_{sup} to train the model.

Then, when using \hat{I} to train the model, \exists a polynomial function $\text{poly}(\cdot, \cdot, \cdot, \cdot)$ such that $\forall \varepsilon, \delta > 0$, for all distribution \mathcal{D} over $\mathcal{X} \times \mathcal{Y}$, then $\forall m \geq \text{poly}(1/\varepsilon, 1/\delta, \text{size}(c))$, we have

$$\mathbb{P}_{S \sim \mathcal{D}^m} [R(h_S) - \min_{h \in \mathcal{H}} R(h) \leq \varepsilon] \geq 1 - \delta. \quad (4)$$

Similarly, there exists a polynomial $\text{poly}_{\text{sup}}(\cdot, \cdot, \cdot, \cdot)$ such that for the above ε, δ and distribution \mathcal{D} , $\forall m \geq \text{poly}_{\text{sup}}(1/\varepsilon, 1/\delta, \text{size}(c))$, we have

$$\mathbb{P}_{S \sim \mathcal{D}^m} [R_{\text{sup}}(h_S) - \min_{h \in \mathcal{H}} R_{\text{sup}}(h) \leq \varepsilon] \geq 1 - \delta. \quad (5)$$

Therefore, let

$$M = \sup \{ \text{poly}(1/\varepsilon, 1/\delta, \text{size}(c)), \text{poly}_{\text{sup}}(1/\varepsilon, 1/\delta, \text{size}(c)) \},$$

then for any $m > M$, both equation (4) and (5) satisfy and our theorem holds.

This theorem suggests that using I_{sup} or \hat{I} to regularize the model may yield similar results. In the next section, we provide an empirical illustration.

Score Distribution Analysis

In this section, we plot the score distribution on CIFAR-10 (Krizhevsky 2009) benchmark using SVHN (Netzer et al. 2011) and CIFAR-100 (Krizhevsky 2009) as the OOD datasets. As shown in Figure A, we can see that in row (a), after applying OAL (Hendrycks, Mazeika, and Dietterich 2019), the standard deviation of the estimated scores on both in-distribution and out-of-distribution datasets are reduced. The accuracy of OOD score estimation is also improved. The same phenomena can be observed on SVHN (Netzer et al. 2011), which is shown in row (b).

Comparisons with Other Training Methods

In this section, we compare OAL with other Outlier Exposure-based and training-based approaches like MCD (Yu and Aizawa 2019), LogitNorm (Wei et al. 2022) and UDG (Yang et al. 2021). We train these methods following the settings given in OpenOOD (Zhang et al. 2024). The resolution of the train and test images are still 224×224 . The train batch size is all set to 128, the validation and test batch size are set to 200.

Table B: Comparisons with other training-based methods on the CIFAR-100 (Krizhevsky 2009) benchmark. We use CIFAR-100 (Krizhevsky 2009) as the in-distribution dataset to train a ResNet-18 (He et al. 2016) using EBO (Liu et al. 2020) score function. \uparrow indicates that the higher the value, the better the OOD performance and vice versa. We report standard deviations across 3 runs of our method. The bold numbers represent the best results.

Methods	OOD Dataset								ID ACC
	Near-OOD		Far-OOD						
	CIFAR-10		MNIST		SVHN		Average		
	FPR@95 ↓	AUROC ↑	FPR@95 ↓	AUROC ↑	FPR@95 ↓	AUROC ↑	FPR@95 ↓	AUROC ↑	
MCD (Yu and Aizawa 2019)	62.82	78.06	46.26	84.87	49.78	83.42	52.95	82.12	75.61
UDG (Yang et al. 2021)	67.12	75.26	26.97	93.24	53.14	79.03	49.08	82.51	70.46
LogitNorm (Wei et al. 2022)	85.08	66.44	67.96	67.38	29.50	92.89	60.85	75.57	74.98
OAL (Ours)	61.50±1.34	79.25±0.30	35.73±3.27	90.25±0.72	43.41±4.11	86.45±2.07	46.88±1.06	85.32±0.53	77.09±0.43

Table C: Comparisons with other training-based methods on the CIFAR-10 (Krizhevsky 2009) benchmark. Here we train a ResNet-18 (He et al. 2016) using EBO (Liu et al. 2020) scoring function. \uparrow indicates that the higher the value, the better the OOD performance and vice versa. We report standard deviations across 3 runs of our method. The bold numbers represent the best results.

Methods	OOD Dataset								ID ACC
	Near-OOD		Far-OOD						
	CIFAR-100		MNIST		SVHN		Average		
	FPR@95 ↓	AUROC ↑	FPR@95 ↓	AUROC ↑	FPR@95 ↓	AUROC ↑	FPR@95 ↓	AUROC ↑	
MCD (Yu and Aizawa 2019)	33.93	90.54	24.48	92.69	14.64	95.90	24.35	93.04	94.16
UDG (Yang et al. 2021)	56.00	81.82	19.42	95.09	62.51	77.05	45.98	84.65	86.39
LogitNorm (Wei et al. 2022)	34.43	90.41	21.91	94.08	10.56	96.99	22.30	93.83	94.60
OAL (Ours)	31.20±0.68	91.63±0.10	5.64±0.71	98.50±0.18	9.03±0.93	97.56±0.39	15.29±0.63	95.89±0.21	95.01±0.14

The results are shown in Table B and C. As shown in Table B and C, our method achieves the best results on both CIFAR-10 and CIFAR-100 (Krizhevsky 2009) benchmarks compared with other training-based methods.

Baselines

To evaluate the post hoc-based baselines, such as MSP (Hendrycks and Gimpel 2017), ODIN (Liang, Li, and Srikant 2018), Gram (Sastry and Oore 2020), EBO (Liu et al. 2020), ReAct (Sun, Guo, and Li 2021), ViM (Wang et al. 2022), KNN (Sun et al. 2022), GEN (Liu, Lochman, and Zach 2023), we directly use the settings given in OpenOOD (Zhang et al. 2024) with the same pre-trained ResNet-18 backbone. Note that the resolution of images is all set to 224×224 . In ODIN, the temperature is set to $T = 1000$. For EBO, the temperature is set to $T = 1$.

For OE (Hendrycks, Mazeika, and Dietterich 2019) and VOS (Du et al. 2022c), MCD (Yu and Aizawa 2019), Logit-Norm (Wei et al. 2022) and UDG (Yang et al. 2021), we also use the settings in OpenOOD (Zhang et al. 2024).

For Dream-OOD (Du et al. 2023) and GAN (Lee et al. 2018), we directly cite the results given in Dream-OOD (Du et al. 2023).

In addition, when reproducing ATOL (Zheng et al. 2023) using the released code, we strictly adhere to the settings in their paper, except for the training device. In ATOL, the authors use A100 GPUs, whereas we employ a single V100 GPU. We report the best results achieved during their 10-epoch training period.

Theoretical Justification for Why OAL Work

In this section, we try to explain why OAL works for OOD detection performance enhancement. Before this, we give the following assumption, which is also used in GEM (Morteza and Li 2022).

Assumption 2. Assume that the ID data follows a mixture of Gaussian distribution with unequal prior.

Specifically, the density function of ID data distribution P^{in} can be written as follows,

$$p^{in}(\mathbf{x}) = \sum_{j=1}^k w_j p_{\mathcal{X}|\mathcal{Y}}^{in}(\mathbf{x}|y_j) \\ = \frac{\sum_{i=1}^k w_j \exp(-\frac{1}{2}(\mathbf{x} - \boldsymbol{\mu}_i)^\top \Sigma^{-1}(\mathbf{x} - \boldsymbol{\mu}_i))}{\sqrt{(2\pi)^d |\Sigma|}}.$$

where \mathbf{x} represents the image sample from input space \mathcal{X} , $\mathcal{Y} = \{y_i\}_{i=1}^k$ is the label space, $\boldsymbol{\mu}_i$ ($i = 1, \dots, k$, k is the number of class) is the mean of class $y_i \in \mathcal{Y}$, w_i is the weight of each class i , and $\Sigma = \sigma^2 \mathbf{I} \in \mathbb{R}^{d \times d}$ is the covariance matrix, σ is the standard deviation value, d is the dimension of the feature space.

Then, from the perspective of generalization error, we can show the following Proposition.

Proposition 1. Denote \mathcal{H} as the hypothesis space on ID data. Let

$$R(h) = \mathbb{E}_{\mathbf{x} \sim \mathcal{D}^{in}} \left[\sum_{i=1}^k \mathbb{I}_{[h(\mathbf{x})]_i \neq [f(\mathbf{x})]_i} \right]$$

as the generalization error of $h \in \mathcal{H}$ on ID data \mathcal{D}^{in} , where $h(x)$ is the predicted value and $f(x)$ is the target value, \mathbb{I} is the indicator function, k is the number of classes. For a score function S , denote the False Positive Rate as $FPR(S)$. Then $FPR(S)$ is bounded by $\inf_{h \in \mathcal{H}} R(h)$.

Proof. For fixed $i \in [1, k]$, $i \in \mathbb{Z}$, the class-conditioned test OOD distribution can be any distribution of the following distribution family:

$$\bigcup_{i=1}^k \{P^{ood}(\mathbf{x}^{ood}|y_i)\} = \bigcup_{i=1}^k \{\mathbf{x}^{ood} : \Pr[\|\mathbf{x}^{ood} - \boldsymbol{\mu}_i\|_2 \leq \tau] \leq \varepsilon_\tau\},$$

where $\tau = \sigma\sqrt{d} + \sigma\gamma + \varepsilon\sqrt{d}$, $\gamma \in (0, \sqrt{d})$, is a parameter that indicates the margin between ID and OOD distributions, ε_τ and ε are arbitrary sufficiently small numbers.

Take $\varepsilon_\tau = \inf_{h \in \mathcal{H}} R(h)$, then we have

$$\begin{aligned} FPR(S) &= \frac{1}{k} \sum_{i=1}^k \mathbb{E}_{\mathbf{x} \sim P^{ood}(\mathbf{x}^{ood}|y_i)} \mathbb{I}[\|\mathbf{x} - \boldsymbol{\mu}_i\|_2 \leq r] \\ &\leq \sup_{1 \leq i \leq k} \mathbb{E}_{\mathbf{x} \sim P^{ood}(\mathbf{x}^{ood}|y_i)} \mathbb{I}[\|\mathbf{x} - \boldsymbol{\mu}_i\|_2 \leq r] \\ &\leq \sup_{1 \leq i \leq k} \mathbb{E}_{\mathbf{x} \sim P^{ood}(\mathbf{x}^{ood}|y_i)} \mathbb{I}[\|\mathbf{x} - \boldsymbol{\mu}_i\|_2 \\ &\quad - \sqrt{d}\varepsilon \leq \sigma\sqrt{d} + \sigma\gamma] \\ &= \sup_{1 \leq i \leq k} \Pr[\|\mathbf{x} - \boldsymbol{\mu}_i\|_2 \leq \tau] \\ &\leq \varepsilon_\tau = \inf_{h \in \mathcal{H}} R(h). \end{aligned}$$

where $r = (1 + \gamma/4\sqrt{d})\hat{\sigma}$ and $\hat{\sigma}^2 = \frac{1}{n} \sum_{i=1}^n \|\mathbf{x}_i - \bar{\mathbf{x}}\|_2^2$.

The above proof implies that the better the model's generalization ability on ID data, the lower its corresponding FPR value will be, which indicates higher OOD detection performance.

Software and Hardware

We run all experiments using Python 3.8.19, Pytorch 1.13.1 and only one V100 GPU.